Environmental Science & Technology Letters

pubs.acs.org/journal/estlcu

Letter

Rapid Increases in Warm-Season Surface Ozone and Resulting Health Impact in China Since 2013

Xiao Lu, Lin Zhang,* Xiaolin Wang, Meng Gao, Ke Li, Yuzhong Zhang, Xu Yue, and Yuanhang Zhang*

Cite This: *Environ. Sci. Technol. Lett.* 2020, 7, 240−247

Read Online

ACCESS | Metrics & More | Article Recommendations | Supporting Information

ABSTRACT: China's nationwide ozone monitoring network initiated in 2013 has observed severe surface ozone pollution. This network, combined with the recent Tropospheric Ozone Assessment Report (TOAR) data set, offers a more comprehensive view on global surface ozone distribution and trends. Here, we report quantitative estimates of the warm-season (April−September) surface ozone trends and resulting health impacts at Chinese cities in 2013−2019. Both the parametric and nonparametric linear trends for 12 ozone metrics relevant to human health and vegetation exposure are derived. We find that all ozone metrics averaged from Chinese urban sites have increased significantly since 2013. The warm-season daily maximum 8-h average (MDA8) ozone levels increased by 2.4 ppb (5.0%) year^{-1}, with over 90% of the sites showing positive trends and 30% with trends larger than 3.0 ppb year^{-1}. These rates are among the fastest trends, even faster in some Chinese cities, compared with the urban ozone trends in any other region worldwide reported in TOAR. Ozone metrics reflecting the cumulative exposure effect on human health and vegetation such as SOMO35 and AOT40 have increased at even faster rates (>10% year^{-1}). We estimate that the total premature respiratory mortalities attributable to ambient MDA8 ozone exposure in 69 Chinese cities are 64,370 in 2019, which has increased by 60% compared to 2013 levels and requires urgent attention.

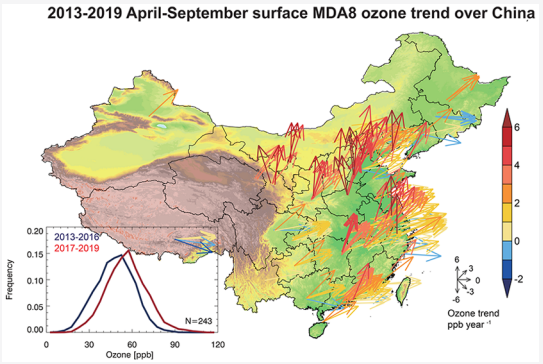

1. INTRODUCTION

Short-term and long-term exposures to ambient ozone, a damaging air pollutant, can contribute to risks of respiratory or circulatory mortality[1−4] and also induce plant cell death and yield reductions.[5,6] In urban regions, ozone is generated rapidly from the sunlight-driven oxidation of carbon monoxide (CO) and volatile organic compounds (VOCs) in the presence of nitrogen oxides (NO_x = NO + NO_2). Urban ozone levels in the United States and Europe have been decreasing or leveling off since the 1990s, dominantly attributed to stringent emission controls of anthropogenic ozone precursors.[7−11] The sparsity of observations before 2013 has hindered our understanding of the historical ozone evolution in China. Some limited measurements at individual surface sites[12−18] and more recently satellite retrievals[19] have unveiled notable ozone increases since the 1990s or 2000s.

The Chinese nationwide air quality monitoring network that became available in 2013 provides the first chance to understand surface ozone levels nationwide in China. This network, combined with the recent Tropospheric Ozone Assessment Report (TOAR) that has archived ozone observational networks in the United States, Europe, Japan, and South Korea up to 2014,[20,21] offers a comprehensive view of the surface ozone in the northern midlatitudes. Lu et al.[22] showed that present-day (2013−2017) urban surface ozone levels in China were significantly higher than those in other regions reported in TOAR. They also found that ozone levels in China for 2016−2017 were higher than those for 2013−2014, likely driven by chemical or meteorological processes.[23−26] However, quantitative analyses on the trend and health impact were not conducted at that time, and neither were addressed in other following studies. Here, with the 7-year (2013−2019) continuous measurements, a robust trend analysis and comparison to global urban ozone trends becomes feasible, using the recent proposed statistical method applied to ozone trend calculation.[27] Such an analysis is very important for assessing the effectiveness of recent emission control measures in China. It also completes and advances our understanding of global ozone trends gained from TOAR in which the data in China were limited.

This study presents a quantitative analysis of the warm-season (April−September) surface ozone trend in China from 2013 to 2019 and comparisons to global urban ozone trends reported in TOAR.[28] The trends are calculated for sites with continuous observations in the 7-year period based on monthly ozone anomalies following the method adopted by Cooper et

Received: March 3, 2020
Revised: March 17, 2020
Accepted: March 18, 2020
Published: March 18, 2020

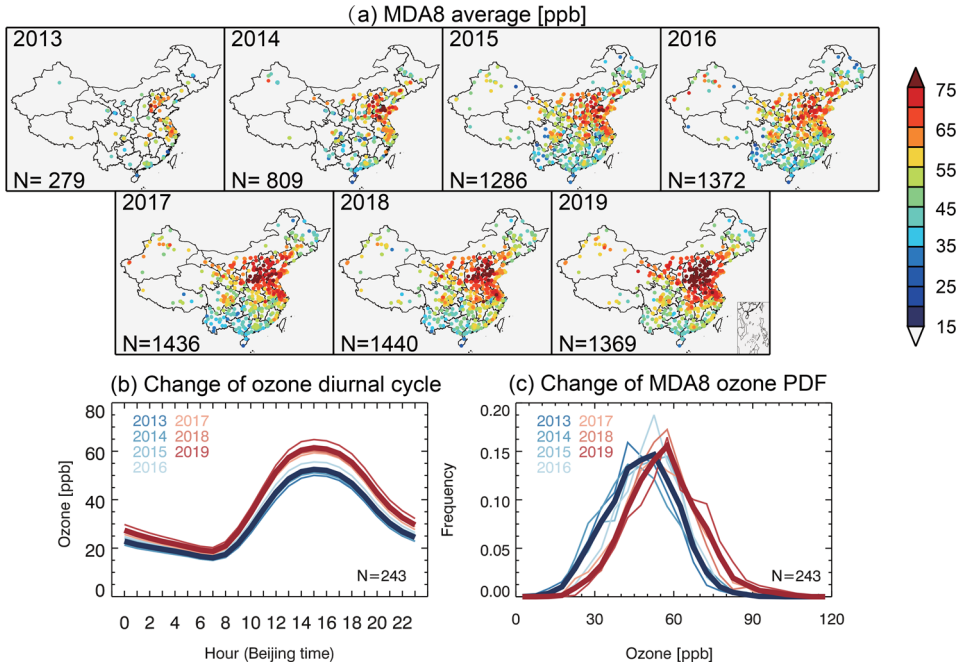

Figure 1. April−September surface ozone in China in 2013−2019. (a) Spatiotemporal distributions of April−September averaged MDA8 ozone. Numbers (N) denote available sites for each year. (b) Ozone diurnal cycles and (c) probability density functions (PDF) of daily MDA8 ozone in April−September from 2013−2019 at 243 Chinese sites. The dark thick red lines represent the ozone levels averaged for 2017−2019, and dark thick blue lines represent values averaged for 2013−2016. Ozone levels for the individual years are shown by the light thin lines.

al.[27] We analyze both the parametric and nonparametric linear trends for a variety of ozone metrics recommended by TOAR.[4] We further estimate the 2013−2019 changes in premature mortality attributable to ambient ozone exposure in Chinese cities.

2. MATERIALS AND METHODS

Ozone Observation. The nationwide hourly ozone observations in Chinese cities are obtained from the China National Environmental Monitoring Center (CNEMC) network (SI, http://106.37.208.233:20035/, access date March 10, 2020). We apply extensive data quality controls to remove unreliable data outliers and to select sites with continuous observations in 2013−2019 for trend analyzes (SI); 243 sites in 69 cities shown in Table S1 and Figure S1 are used. To provide a global view, we also use the warm-season surface ozone trends in 2005−2014 periods at global ozone monitoring sites archived in the TOAR data set (10.1594/PANGAEA.876108, access date March 10, 2020).[20,21]

Ozone Metrics. We include a total of 12 metrics (Table S2) to characterize ozone pollution and its impacts on human health and ecosystems following the TOAR definition.[4] These metrics include standard statistics such as the fifth- (Perc5), 50th- (median), and 95th-percentile (Perc95) level, daytime and nighttime averages, and daily maximum 1-h (MDA1) and 8-h averages (MDA8). MDA1 and MDA8 are used for assessing ozone air quality and in cohort studies examining the responses of human health to ozone exposure.[1−3] NDGT70 (total number of days with MDA8 > 70 ppb) and SOMO35 metrics (sum of daily MDA8 ozone over 35 ppb) are used to estimate the acute or cumulative health exposure.[4] AOT40 and W126 metrics estimate ozone damages to natural vegetation.[4] We derived all metrics from the hourly measurements (those have been filtered by data quality control procedures) following the TOAR data completeness requirements and procedures. Metrics are calculated both for April−September aggregation (in consistent with TOAR) and for each month (for trend analyses).

Trend Analyses. A recent study on long-term global ozone trends by Cooper et al.[27] shows that trends calculated from monthly averages can be less accurate than those from monthly anomalies when there are missing data.[27] They proposed a method based on monthly anomalies for ozone trend analysis, which has been previously used to calculate trends in time series of variables with seasonal cycles and autocorrelation.[29−31] Following their method, we calculate trends based on the anomalies of monthly mean ozone metrics rather than the April−September averages. The monthly anomalies of each ozone metric are derived as the difference between the individual monthly mean values and the 2013−2019 monthly means. The parametric linear trends are calculated using the generalized least-squares method with autoregression[27]

$$y_t = b + kt + \alpha \cos\left(\frac{2\pi M}{6}\right) + \beta \sin\left(\frac{2\pi M}{6}\right) + R_t$$

where y_t represents the monthly anomaly, t is the monthly index from April 2013 to September 2019 (i.e., from 1 to 42), b denotes the intercept, k is the linear trend, α and β are coefficients for a 6-month harmonic series (M ranges from 1 to 6) to account for potentially remaining seasonal signals in y_t, and $R_t = \rho R_{t-1} + \epsilon_t$ accounts for autocorrelation with ϵ_t representing a normal random error series. Trends and p-values are reported with a 95% confidence level. We also use the nonparametric Mann−Kendall (M-K) test[32] and Theil−-Sen estimator[33,34] to calculate the magnitude and significance of trends, which has been applied in TOAR and other ozone trend studies.[4,9,12,16]

Premature Respiratory Mortalities Attributable to Ozone Exposure. We estimate the total premature respiratory mortalities attributable to ambient ozone exposure

https://dx.doi.org/10.1021/acs.estlett.0c00171
Environ. Sci. Technol. Lett. 2020, 7, 240−247

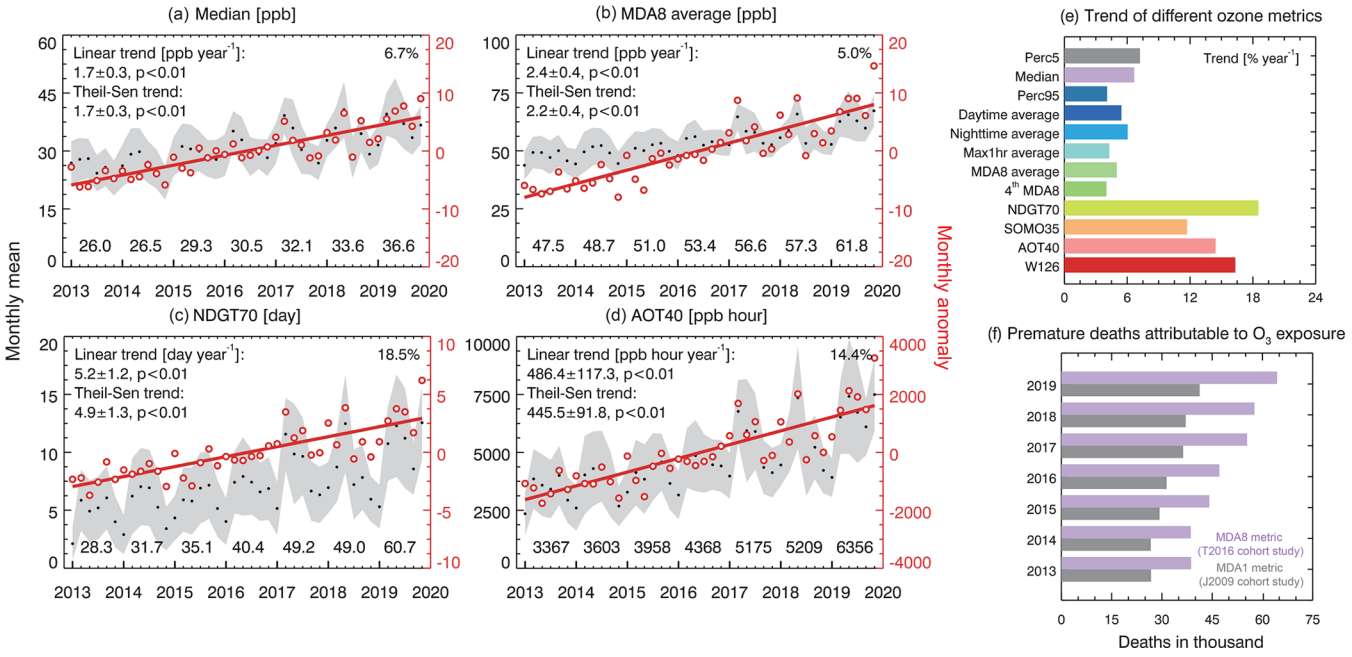

Figure 2. Trends of the different ozone metrics and premature respiratory mortalities due to ozone exposure from April−September 2013−2019 at 243 Chinese ozone monitoring sites (Table S1, Figure S1). (a)−(d) Time series of the average (black dots, left axis) and anomaly (red circle, right axis) of four monthly mean ozone metrics (Median, MDA8, NGDT70, AOT40; others are shown in Figure S3) from April 2013 to September 2019. Gray shading represents the range of mean value ± the 50% standard deviation across all sites for each month. The solid line represents the linear fitted curve. The absolute annual linear trend, Theil−Sen trend, and percentage of annual trend (% per year, calculated as the linear trend divided by the 2013 mean values) are shown inset. The numbers denotes the warm-season averaged/aggregated values of each metric. (e) Annual trend in percentage (% per year) for all 12 ozone metrics. (f) Changes in total premature respiratory mortalities due to ozone exposure in April−September 2013−2019 at 69 Chinese cities based on the Jerrett et al.[1] cohort study using the MDA1 metric (J2009 cohort study, gray bars) and the Turner et al.[2] cohort study using the MDA8 metric (T2016 cohort study, purple bars).

at 69 Chinese cities from 2013−2019, based on the exposure−response relationship used in the most recent Global Burden of Deceases (GBD) study[35] and described in Seltzer et al.[36] as

$$\Delta x = \begin{cases} 0 & (\text{if [Ozone]} \le \text{TMREL}) \\ [\text{Ozone}] - \text{TMREL} & (\text{if [Ozone]} > \text{TMREL}) \end{cases}$$

$$\text{HR} = \exp(\beta \Delta \text{Y})$$

$$\text{AF} = 1 - \exp(-\beta \Delta \text{x})$$

$$\Delta\text{Mort} = y_o \times AF \times \text{Pop}$$

Here, we use both the April−September mean MDA1 and MDA8 ozone metrics according to two cohort studies.[1,2] MDA1 and MDA8 at city levels are calculated by averaging available monitoring sites within each city. TMREL represents the theoretical minimum risk exposure level, which is 33.3 ppb for April−September MDA1[1] and 29.1 ppb for April−September MDA8[2] (Table S3). Δx is ozone exposure relative to TMREL. β is the exposure−response factor derived from the reported hazard ratio (HR) to incremental changes in ozone exposure (ΔY, 10 ppb for both metrics). HR values for respiratory diseases are 1.040 (95% confidence interval (CI): 1.013, 1.067) for MDA1[1] and 1.08 (1.06, 1.11) for MDA8[2] (Table S3). AF is the attributable fraction representing the disease burden attributable to ozone exposure. y_o is the baseline mortality rate for respiratory diseases for all ages and genders obtained from the GHDx (Global Heath Data Exchange) database (available for 2013−2017, and values of 2017 are used afterward). GHDx only provides national y_o values for mainland China, and we apply the provincial information on y_o values as shown in Figure S2 following Gao et al.[37] Pop is population at an individual city for year 2017 obtained from the government annual report. The product of AF, y_o, and Pop yields the number of premature respiratory mortalities at an individual city (ΔMort).

3. RESULTS AND DISCUSSION

Figure 1 shows the MDA8 ozone values averaged from April−September at all available sites for each year in 2013−2019. Locations and definitions of the key regions are shown in Figure S1 and Table S1. Sites with ozone levels exceeding 60 ppb are widely distributed in eastern and central China and the Sichuan Basin (SCB) where intensive anthropogenic emissions are located. Distinct exacerbation of ozone pollution can be seen from 2013 to 2019. In years before 2015, sites with MDA8 ozone greater than 60 ppb are concentrated near the North China Plain (NCP) and the Yangtze River Delta (YRD) megacity clusters. Since 2016, ozone hot spots extend westward to the Fenwei Plain (FWP) and southward to the central Yangtze River Plain (CYR). The percentage of sites with April−September mean MDA8 ozone higher than 60 ppb increases from 11.1% in 2013 to 35.7% in 2017 and further to 49.2% in 2019. There are 150 out of 1369 (11%) sites in 2019 with the April−September mean MDA8 ozone higher than 75 ppb, approximately the Chinese grade II national air quality standard.

We analyze the surface ozone trends in China from 2013−2019 at the 243 sites with continuous observations in these 7-year period. Figure 2 and Figure S3 present the time series of the anomalies of the monthly mean ozone metrics averaged

https://dx.doi.org/10.1021/acs.estlett.0c00171
Environ. Sci. Technol. Lett. 2020, 7, 240−247

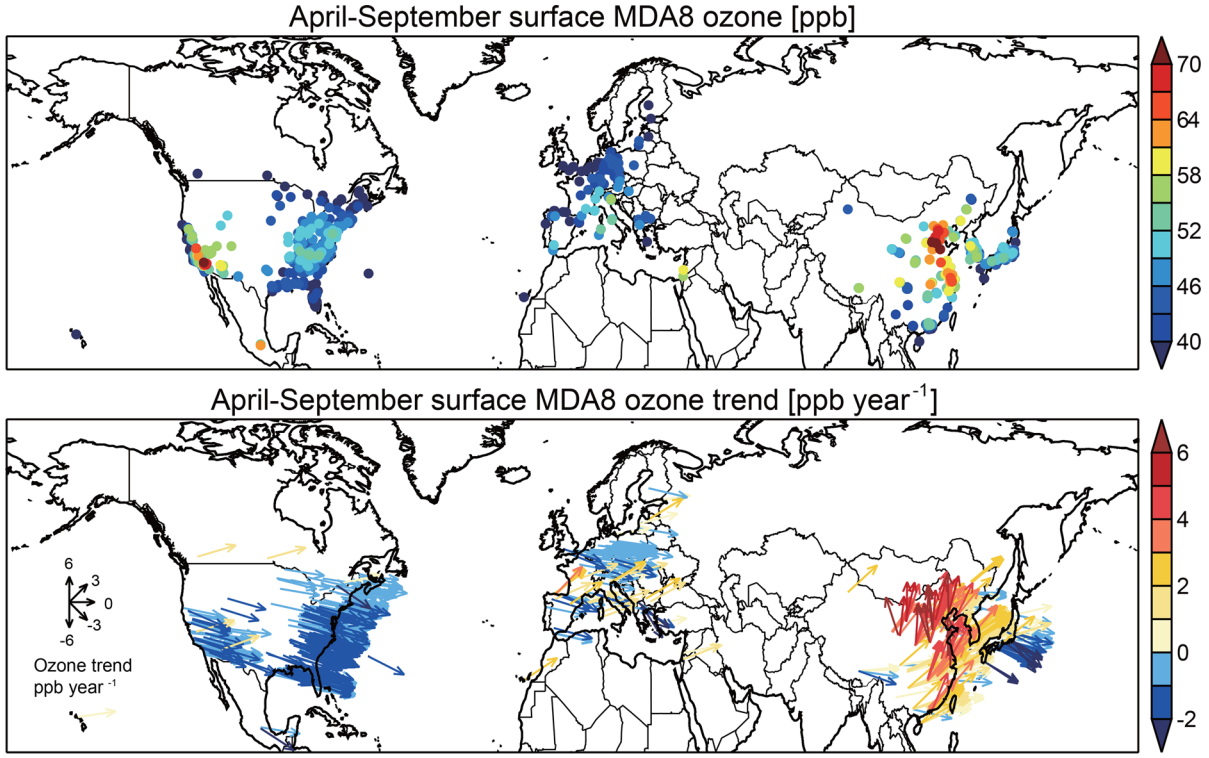

Figure 3. Comparison of April−September mean MDA8 ozone concentrations (top panel) and trends (bottom panel) in Chinese urban sites and TOAR sites. Mean MDA8 ozone values are averages from 2013−2019 for Chinese sites and 2010−2014 for other regions. Trends are estimated using the Theil−Sen method from 2013−2019 for Chinese sites and from 2005−2014 for other regions. Both directions and colors of the vectors indicate the ozone change rates in ppb year^{-1} as adapted with permission under a Creative Commons CC-BY license from ref 61.

from the 243 sites, and Figures S4−S5 show their spatial patterns. We find that ozone levels at Chinese cities are increasing at all selected percentiles. Ozone levels at the fifth, 50th, and 95th percentiles increase at, respectively, 0.4 (7%), 1.7 (7%), and 2.8 (4%) ppb year^{-1} (all with $p < 0.05$) averaged from these sites based on the linear trend estimate (Figure 2 and Figure S3). More than 90% of the 243 sites show increases in the median and Perc95 ozone levels (and 60% with $p < 0.05$) (Table S4 and Figures S4−S5). The parametric linear trend estimates are consistent with the M-K test and Theil−Sen trend estimates. Additional analyses for ozone trends in 2014−2019 at 728 available sites show similar magnitudes and spatial patterns of the positive trend (Table S5).

We can also see significant increases in both the daytime and nighttime mean ozone levels at more than 90% of sites. The averaged daytime mean ozone (2.1 ppb year^{-1}, $p < 0.05$) shows a larger trend in magnitude than the nighttime ozone (1.3 ppb year^{-1}, $p < 0.05$), leading to a larger ozone diurnal contrast. As shown in Figure 1b, the mean April−September mean ozone diurnal contrast increases from 36 ppb for 2013−2016 to 43 ppb for 2017−2019. We find some exceptions with reduced diurnal contrasts such as at the downtown site of Shanghai megacity where nighttime ozone is highly sensitive to NO_x levels.[38] The ozone increases at all percentiles, and both daytime and nighttime averages at most Chinese cities are distinctly different from those in the United States and Europe, where ozone levels are typically decreasing for daytime or high ozone values (e.g., 95th percentile), but increasing for nighttime or low values (e.g., fifth percentile) due to the weakened ozone titration.[7,8,39,40]

The April−September mean MDA8 and MDA1 ozone levels increase by 2.4 ppb year^{-1} (4%−5% year^{-1}, $p < 0.05$) averaged from all sites (Figure 2), with more than 90% of the sites showing positive trends (Figure S4). The increases also exhibit interannual variabilities, for example, years 2017 and 2019 showed MDA8 increases by more than 3 ppb compared to their previous years. Regionally, the NCP (55 sites) and FWP (Xi'an city, nine sites) regions show the largest increases in MDA8 (3.3 and 4.1 ppb year^{-1}, respectively) compared to other regions (Table S6). These rates are remarkably fast from a global perspective. Figure 3 compares the MDA8 ozone values and trends for 2013−2019 at Chinese sites with those urban and suburban sites archived in TOAR for 2005−2014.[28] TOAR reports urban ozone increases in South Korea, Japan, and South Europe, with only three sites showing MDA8 ozone trends greater than 3 ppb year^{-1} in 2005−2014. These sites have moderate MDA8 ozone levels of less than 50 ppb (Figure 3). By contrast, 85 of the 243 Chinese sites are experiencing MDA8 ozone increases at more than 3 ppb year^{-1} from 2013 to 2019, with MDA8 at these sites typically higher than 60 ppb. Even larger rates of more than 5 ppb year^{-1} are seen at some sites in the NCP and FWP city clusters. Our analyses suggest both higher ozone levels and faster increasing rates in China than other regions in the world covered in the monitoring networks.

We now assess the influence of increasing ozone exposures on human health in China. As shown by MDA8 ozone probability distribution functions (PDF) averaged from the 243 Chinese urban sites (Figure 1c), the accumulated probability of a MDA8 ozone larger than 35 (70) ppb increases from 83% (5.3%) in 2013−2016 to 94% (18%) in 2017−2019. As a result, the SOMO35 and NDGT70 ozone metrics enhance at rates of 11.7% and 18.5% year^{-1}, indicating significant increases in the duration, magnitude, and frequency

https://dx.doi.org/10.1021/acs.estlett.0c00171
Environ. Sci. Technol. Lett. 2020, 7, 240−247

of hazardous ozone episodes in China. On the basis of the warm-season MDA8 and MDA1 metrics, we find that the 2013−2019 mean premature respiratory mortalities attributable to ambient ozone exposure from the 69 cities are 49,430 (95% CI: 34,350−64,610) and 32,690 (13,560−51,380). Regionally, larger premature mortalities are shown in cities in eastern China due to high ozone levels and a large population and cities in the SCB due to a high baseline mortality rate for respiratory diseases (Figure S2). These values are comparable to previous observation-based estimates from Chinese cities which used different ozone metrics and baseline mortalities[41] but lower than model-based estimates which typically focused on larger domains.[36,42,43] Nevertheless, both metrics show that the ozone-induced premature respiratory mortalities have increased significantly by about 60% (8.6% $year^{-1}$) from 2013 (38,710 for MDA8 and 26,760 for MDA1) to 2019 (64,370 for MDA8 and 41,270 for MDA1) (Figure 2f). Additional analyses using the annual mean MDA8 metrics yield similar trends (Table S3). These mortality increases can be dominantly (93%) attributed to increases in ozone levels with the rest to increases in the baseline mortality rate. The effects of changes in population at these cities on ozone-induced mortalities are not considered in our estimates.

As for metrics of vegetation exposure, AOT40 and W126 values have been increasing at rates of 14.4% and 16.3% per $year^{-1}$ from 2013−2019, respectively, and both are doubled in 2019 compared to their 2013 levels (Figure 2 and Figure S3). The large rates of AOT40 and W126 also reflect the cumulative effects of an upward shift of ozone concentration PDF (Figure 1c) that increases both the high end ozone levels and the duration of daytime hourly ozone exceeding 40 ppb (~1-h extension in 2017−2019 relative to 2013−2016, Figure 1b). Regionally, large AOT40 and W126 increases are found in NCP, CYP, and FWP regions, causing large ozone damages on crop yield and primary productivity as reported in previous studies.[44−47]

Identifying the drivers of rapid ozone increases since 2013 is crucial for effectively controlling the ozone pollution in China. Recent attempts have proposed a number of candidates, but a consensus has not reached. The nationwide emission control measures have decreased the anthropogenic NO_x emission by 21% in 2017 compared to 2013, but VOCs emissions have slightly increased.[48] As ozone chemical productions in NCP and YRD city clusters are likely VOC-limited or mixed-sensitive,[38,49−51] increases in VOCs emissions could have enhanced ozone levels in these regions. While satellite observations show general decreases of April−September tropospheric NO_2 columns from 2013 to 2019 (Figure S6), two years, 2017 and 2019, which recorded the largest national mean ozone enhancements relative to their previous years (Figure 2b), observe increases in tropospheric NO_2 columns, and the causes are still unclear. Another potential chemical driver of the ozone increases can be concurrent decreases in the $PM_{2.5}$ level[52,53] that may have weakened the aerosol sink of hydroperoxy radicals and increased solar radiation.[23,24,54] Li et al.[23] estimated that the combined effects of changes in emissions and $PM_{2.5}$ levels could lead to summertime MDA8 ozone enhancements of approximately 1 ppb $year^{-1}$ in NCP during 2013−2017, which was insufficient to explain the observed trend (~3.3 ppb $year^{-1}$) as revealed in this study. Recent studies have also identify the important roles of weather patterns controlling ozone pollution episodes[55−58,58−60] and meteorological contributions to the ozone increases via physical and chemical processes.[25,26] Lu et al.[26] found that meteorology rather than anthropogenic emission change was the dominant factor in driving the ozone increase in 2017 compared to 2016, reflecting strong influences of meteorological patterns on the interannual variability of surface ozone in China.

We conclude that there are widespread and rapid surface ozone increases in Chinese cities during 2013−2019. More than 90% of the 243 urban sites show positive trends using various ozone metrics, and about 60% of the sites show trends with $p < 0.05$. Metrics such as MDA1, MDA8, Perc95, and 4MDA8 which focus on the mean or the high ozone pollution episodes increase by about 2.4−2.7 ppb $year^{-1}$. Metrics such as SOMO35, AOT40, and W126 that estimate the cumulative exposure effects of ozone to human health and vegetation have been increasing at even faster rates (over 10% $year^{-1}$). The premature respiratory mortalities due to ozone exposure in Chinese cities have increased by 60% in 2019 compared to 2013 levels. Recent studies based on chemical transport models or statistical analyses have not been able to reproduce such rapid increases in surface ozone in China since 2013. Further studies are in urgent need to disentangle the underlying chemical and meteorological drivers.

■ ASSOCIATED CONTENT

Supporting Information

The Supporting Information is available free of charge at https://pubs.acs.org/doi/10.1021/acs.estlett.0c00171.

Additional text for the ozone observation and data quality control. Tables and figures describing the site locations, definition of ozone metrics, calculation of the ozone health exposure, trends for all ozone metrics and their spatial distributions, and changes in observed tropospheric NO_2 columns. (PDF)

■ AUTHOR INFORMATION

Corresponding Authors

Lin Zhang − *Laboratory for Climate and Ocean-Atmosphere Studies, Department of Atmospheric and Oceanic Sciences, School of Physics, Peking University, Beijing 100871, China;* orcid.org/0000-0003-2383-8431; Email: zhanglg@pku.edu.cn

Yuanhang Zhang − *State Key Joint Laboratory of Environmental Simulation and Pollution Control, College of Environmental Sciences and Engineering, Peking University, Beijing 100871, China*; Email: yhzhang@pku.edu.cn

Authors

Xiao Lu − *Laboratory for Climate and Ocean-Atmosphere Studies, Department of Atmospheric and Oceanic Sciences, School of Physics, Peking University, Beijing 100871, China;* orcid.org/0000-0002-5989-0912

Xiaolin Wang − *Laboratory for Climate and Ocean-Atmosphere Studies, Department of Atmospheric and Oceanic Sciences, School of Physics, Peking University, Beijing 100871, China*

Meng Gao − *Department of Geography, Hong Kong Baptist University, Hong Kong 999077, China;* orcid.org/0000-0002-8657-3541

Ke Li − *John A. Paulson School of Engineering and Applied Sciences, Harvard University, Cambridge, Massachusetts 02138, United States;* orcid.org/0000-0002-9181-3562

https://dx.doi.org/10.1021/acs.estlett.0c00171
Environ. Sci. Technol. Lett. 2020, 7, 240−247

Yuzhong Zhang − *School of Engineering, Westlake University, Hangzhou 310024, Zhejiang Province, China; Institute of Advanced Technology, Westlake Institute for Advanced Study, Hangzhou 310024, Zhejiang Province, China*

Xu Yue − *Jiangsu Key Laboratory of Atmospheric Environment Monitoring and Pollution Control, Collaborative Innovation Center of Atmospheric Environment and Equipment Technology, School of Environmental Science and Engineering, Nanjing University of Information Science & Technology (NUIST), Nanjing 210044, China*

Complete contact information is available at: https://pubs.acs.org/10.1021/acs.estlett.0c00171

Notes

The authors declare no competing financial interest.

■ ACKNOWLEDGMENTS

This work is supported by the National Key Research and Development Program of China (2017YFC0210102) and the National Natural Science Foundation of China (41922037). The authors acknowledge the Tropospheric Ozone Assessment Report (TOAR) initiative for providing the surface ozone data used in this study. We thank Dr. Owen Cooper, Dr. Kai-Lan Chang at NOAA Earth System Research Laboratory, and Dr. Martin G. Schultz at Jülich Supercomputing Centre for useful suggestions in trend calculation and support in TOAR data application. We thank Dr. Karl Seltzer at Duke University for useful suggestions on health impact estimates.

■ REFERENCES

(1) Jerrett, M.; Burnett, R. T.; Pope, C. A., 3rd; Ito, K.; Thurston, G.; Krewski, D.; Shi, Y.; Calle, E.; Thun, M. Long-term ozone exposure and mortality. *N. Engl. J. Med.* **2009**, *360*, 1085−95.

(2) Turner, M. C.; Jerrett, M.; Pope, C. A.; Krewski, D.; Gapstur, S. M.; Diver, W. R.; Beckerman, B. S.; Marshall, J. D.; Su, J.; Crouse, D. L.; Burnett, R. T. Long-Term Ozone Exposure and Mortality in a Large Prospective Study. *Am. J. Respir. Crit. Care Med.* **2016**, *193*, 1134−42.

(3) Malley, C. S.; Henze, D. K.; Kuylenstierna, J. C. I.; Vallack, H. W.; Davila, Y.; Anenberg, S. C.; Turner, M. C.; Ashmore, M. R. Updated Global Estimates of Respiratory Mortality in Adults > /=30Years of Age Attributable to Long-Term Ozone Exposure. *Environ. Health Perspect.* **2017**, *125*, 087021.

(4) Lefohn, A. S.; Malley, C. S.; Smith, L.; Wells, B.; Hazucha, M.; Simon, H.; Naik, V.; Mills, G.; Schultz, M. G.; Paoletti, E.; De Marco, A.; Xu, X.; Zhang, L.; Wang, T.; Neufeld, H. S.; Musselman, R. C.; Tarasick, D.; Brauer, M.; Feng, Z.; Tang, H.; Kobayashi, K.; Sicard, P.; Solberg, S.; Gerosa, G. Tropospheric ozone assessment report: Global ozone metrics for climate change, human health, and crop/ecosystem research. *Elem Sci. Anth* **2018**, *6*, 28.

(5) Ainsworth, E. A.; Yendrek, C. R.; Sitch, S.; Collins, W. J.; Emberson, L. D. The effects of tropospheric ozone on net primary productivity and implications for climate change. *Annu. Rev. Plant Biol.* **2012**, *63*, 637−61.

(6) Mills, G.; Pleijel, H.; Malley, C. S.; Sinha, B.; Cooper, O. R.; Schultz, M. G.; Neufeld, H. S.; Simpson, D.; Sharps, K.; Feng, Z.; Gerosa, G.; Harmens, H.; Kobayashi, K.; Saxena, P.; Paoletti, E.; Sinha, V.; Xu, X. Tropospheric Ozone Assessment Report: Present-day tropospheric ozone distribution and trends relevant to vegetation. *Elem Sci. Anth* **2018**, *6*, 47.

(7) Cooper, O. R.; Gao, R.-S.; Tarasick, D.; Leblanc, T.; Sweeney, C. Long-term ozone trends at rural ozone monitoring sites across the United States, 1990−2010. *J. Geophys. Res.* **2012**, *117*, D22307.

(8) Simon, H.; Reff, A.; Wells, B.; Xing, J.; Frank, N. Ozone trends across the United States over a period of decreasing NOx and VOC emissions. *Environ. Sci. Technol.* **2015**, *49*, 186−95.

(9) Chang, K.-L.; Petropavlovskikh, I.; Copper, O. R.; Schultz, M. G.; Wang, T. Regional trend analysis of surface ozone observations from monitoring networks in eastern North America, Europe and East Asia. *Elem Sci. Anth* **2017**, *5*, 50.

(10) Lin, M.; Horowitz, L. W.; Payton, R.; Fiore, A. M.; Tonnesen, G. US surface ozone trends and extremes from 1980 to 2014: quantifying the roles of rising Asian emissions, domestic controls, wildfires, and climate. *Atmos. Chem. Phys.* **2017**, *17*, 2943−2970.

(11) Yan, Y.; Pozzer, A.; Ojha, N.; Lin, J.; Lelieveld, J. Analysis of European ozone trends in the period 1995−2014. *Atmos. Chem. Phys.* **2018**, *18*, 5589−5605.

(12) Wang, T.; Dai, J.; Lam, K. S.; Nan Poon, C.; Brasseur, G. P. Twenty-Five Years of Lower Tropospheric Ozone Observations in Tropical East Asia: The Influence of Emissions and Weather Patterns. *Geophys. Res. Lett.* **2019**, *46*, 11463−11470.

(13) Wang, T.; Wei, X. L.; Ding, A. J.; Poon, C. N.; Lam, K. S.; Li, Y. S.; Chan, L. Y.; Anson, M. Increasing surface ozone concentrations in the background atmosphere of Southern China, 1994−2007. *Atmos. Chem. Phys.* **2009**, *9*, 6217−6227.

(14) Ma, Z.; Xu, J.; Quan, W.; Zhang, Z.; Lin, W.; Xu, X. Significant increase of surface ozone at a rural site, north of eastern China. *Atmos. Chem. Phys.* **2016**, *16*, 3969−3977.

(15) Sun, L.; Xue, L.; Wang, T.; Gao, J.; Ding, A.; Cooper, O. R.; Lin, M.; Xu, P.; Wang, Z.; Wang, X.; Wen, L.; Zhu, Y.; Chen, T.; Yang, L.; Wang, Y.; Chen, J.; Wang, W. Significant increase of summertime ozone at Mount Tai in Central Eastern China. *Atmos. Chem. Phys.* **2016**, *16*, 10637−10650.

(16) Xu, W.; Lin, W.; Xu, X.; Tang, J.; Huang, J.; Wu, H.; Zhang, X. Long-term trends of surface ozone and its influencing factors at the Mt Waliguan GAW station, China - Part 1: Overall trends and characteristics. *Atmos. Chem. Phys.* **2016**, *16*, 6191−6205.

(17) Chen, Z.; Zhuang, Y.; Xie, X.; Chen, D.; Cheng, N.; Yang, L.; Li, R. Understanding long-term variations of meteorological influences on ground ozone concentrations in Beijing During 2006−2016. *Environ. Pollut.* **2019**, *245*, 29−37.

(18) Cheng, N.; Li, R.; Xu, C.; Chen, Z.; Chen, D.; Meng, F.; Cheng, B.; Ma, Z.; Zhuang, Y.; He, B.; Gao, B. Ground ozone variations at an urban and a rural station in Beijing from 2006 to 2017: Trend, meteorological influences and formation regimes. *J. Cleaner Prod.* **2019**, *235*, 11−20.

(19) Shen, L.; Jacob, D. J.; Liu, X.; Huang, G.; Li, K.; Liao, H.; Wang, T. An evaluation of the ability of the Ozone Monitoring Instrument (OMI) to observe boundary layer ozone pollution across China: application to 2005−2017 ozone trends. *Atmos. Chem. Phys.* **2019**, *19*, 6551−6560.

(20) Schultz, M. G.; Schröder, S.; Lyapina, O.; Cooper, O.; Galbally, I.; Petropavlovskikh, I.; Von Schneidemesser, E.; Tanimoto, H.; Elshorbany, Y.; Naja, M.; Seguel, R.; Dauert, U.; Eckhardt, P.; Feigenspahn, S.; Fiebig, M.; Hjellbrekke, A.-G.; Hong, Y.-D.; Christian Kjeld, P.; Koide, H.; Lear, G.; Tarasick, D.; Ueno, M.; Wallasch, M.; Baumgardner, D.; Chuang, M.-T.; Gillett, R.; Lee, M.; Molloy, S.; Moolla, R.; Wang, T.; Sharps, K.; Adame, J. A.; Ancellet, G.; Apadula, F.; Artaxo, P.; Barlasina, M.; Bogucka, M.; Bonasoni, P.; Chang, L.; Colomb, A.; Cuevas, E.; Cupeiro, M.; Degorska, A.; Ding, A.; Fröhlich, M.; Frolova, M.; Gadhavi, H.; Gheusi, F.; Gilge, S.; Gonzalez, M. Y.; Gros, V.; Hamad, S. H.; Helmig, D.; Henriques, D.; Hermansen, O.; Holla, R.; Huber, J.; Im, U.; Jaffe, D. A.; Komala, N.; Kubistin, D.; Lam, K.-S.; Laurila, T.; Lee, H.; Levy, I.; Mazzoleni, C.; Mazzoleni, L.; McClure-Begley, A.; Mohamad, M.; Murovic, M.; Navarro-Comas, M.; Nicodim, F.; Parrish, D.; Read, K. A.; Reid, N.; Ries, L.; Saxena, P.; Schwab, J. J.; Scorgie, Y.; Senik, I.; Simmonds, P.; Sinha, V.; Skorokhod, A.; Spain, G.; Spangl, W.; Spoor, R.; Springston, S. R.; Steer, K.; Steinbacher, M.; Suharguniyawan, E.; Torre, P.; Trickl, T.; Weili, L.; Weller, R.; Xu, X.; Xue, L.; Zhiqiang, M. Tropospheric Ozone Assessment Report: Database and Metrics

Data of Global Surface Ozone Observations. *Elem Sci. Anth* **2017**, *5*, 58.
(21) Schultz, M. G.; Schroder, S.; Lyapina, O.; Cooper, O.; Galbally, I.; Petropavlovskikh, I.; Von Schneidemesser, E.; Tanimoto, H.; Elshorbany, Y.; Naja, M.; Seguel, R.; Dauert, U.; Eckhardt, P.; Feigenspahn, S.; Fiebig, M.; Hjellbrekke, A.-G.; Hong, Y.-D.; Christian Kjeld, P.; Koide, H.; Lear, G.; Tarasick, D.; Ueno, M.; Wallasch, M.; Baumgardner, D.; Chuang, M.-T.; Gillett, R.; Lee, M.; Molloy, S.; Moolla, R.; Wang, T.; Sharps, K.; Adame, J. A.; Ancellet, G.; Apadula, F.; Artaxo, P.; Barlasina, M.; Bogucka, M.; Bonasoni, P.; Chang, L.; Colomb, A.; Cuevas, E.; Cupeiro, M.; Degorska, A.; Ding, A.; Frohlich, M.; Frolova, M.; Gadhavi, H.; Gheusi, F.; Gilge, S.; Gonzalez, M. Y.; Gros, V.; Hamad, S. H.; Helmig, D.; Henriques, D.; Hermansen, O.; Holla, R.; Huber, J.; Im, U.; Jaffe, D. A.; Komala, N.; Kubistin, D.; Lam, K.-S.; Laurila, T.; Lee, H.; Levy, I.; Mazzoleni, C.; Mazzoleni, L.; McClure-Begley, A.; Mohamad, M.; Murovic, M.; Navarro-Comas, M.; Nicodim, F.; Parrish, D.; Read, K. A.; Reid, N.; Ries, L.; Saxena, P.; Schwab, J. J.; Scorgie, Y.; Senik, I.; Simmonds, P.; Sinha, V.; Skorokhod, A.; Spain, G.; Spangl, W.; Spoor, R.; Springston, S. R.; Steer, K.; Steinbacher, M.; Suharguniyawan, E.; Torre, P.; Trickl, T.; Weili, L.; Weller, R.; Xu, X.; Xue, L.; Zhiqiang, M. Tropospheric Ozone Assessment Report, links to Global surface ozone datasetsx. *PANGAEA* **2017**, *na*, 5.
(22) Lu, X.; Hong, J.; Zhang, L.; Cooper, O. R.; Schultz, M. G.; Xu, X.; Wang, T.; Gao, M.; Zhao, Y.; Zhang, Y. Severe Surface Ozone Pollution in China: A Global Perspective. *Environ. Sci. Technol. Lett.* **2018**, *5*, 487−494.
(23) Li, K.; Jacob, D. J.; Liao, H.; Shen, L.; Zhang, Q.; Bates, K. H. Anthropogenic drivers of 2013−2017 trends in summer surface ozone in China. *Proc. Natl. Acad. Sci. U. S. A.* **2019**, *116*, 422−427.
(24) Li, K.; Jacob, D. J.; Liao, H.; Zhu, J.; Shah, V.; Shen, L.; Bates, K. H.; Zhang, Q.; Zhai, S. A two-pollutant strategy for improving ozone and particulate air quality in China. *Nat. Geosci.* **2019**, *12*, 906−910.
(25) Liu, J.; Wang, L.; Li, M.; Liao, Z.; Sun, Y.; Song, T.; Gao, W.; Wang, Y.; Li, Y.; Ji, D.; Hu, B.; Kerminen, V.-M.; Wang, Y.; Kulmala, M. Quantifying the impact of synoptic circulation patterns on ozone variability in northern China from April to October 2013−2017. *Atmos. Chem. Phys.* **2019**, *19*, 14477−14492.
(26) Lu, X.; Zhang, L.; Chen, Y.; Zhou, M.; Zheng, B.; Li, K.; Liu, Y.; Lin, J.; Fu, T.-M.; Zhang, Q. Exploring 2016−2017 surface ozone pollution over China: source contributions and meteorological influences. *Atmos. Chem. Phys.* **2019**, *19*, 8339−8361.
(27) Cooper, O. R., Schultz, M. G., Schröder, S., Chang, K. L., Benítez, G. C., Cuevas, E., Fröhlich, M., Galbally, I. E., Kubistin, D., Lu, X., McClure-Begley, A., Molloy, S., Nédélec, P., O'Brien, J., Oltmans, S. J., Petropavlovskikh, I., Ries, L., Senik, I., Sjöberg, K., Sverre Solberg, S., Spain, T. G., Spangl, W., Martin Steinbacher, M., David Tarasick, D., Thouret, V., Xu, X., et al. Multi-decadal surface ozone trends at globally distributed remote locations. In *22nd Conference on Atmospheric Chemistry*; Boston, MA, 16 January 2020.
(28) Fleming, Z. L.; Doherty, R. M.; Von Schneidemesser, E.; Malley, C. S.; Cooper, O. R.; Pinto, J. P.; Colette, A.; Xu, X.; Simpson, D.; Schultz, M. G.; Lefohn, A. S.; Hamad, S.; Moolla, R.; Solberg, S.; Feng, Z. Tropospheric Ozone Assessment Report: Present-day ozone distribution and trends relevant to human health. *Elem Sci. Anth* **2018**, *6*, 12.
(29) Cochrane, D.; Orcutt, G. H. Application of Least Squares Regression to Relationships Containing Auto- Correlated Error Terms. *J. Am. Stat. Assoc.* **1949**, *44*, 32.
(30) Weatherhead, E. C.; Reinsel, G. C.; Tiao, G. C.; Meng, X.-L.; Choi, D.; Cheang, W.-K.; Keller, T.; DeLuisi, J.; Wuebbles, D. J.; Kerr, J. B.; Miller, A. J.; Oltmans, S. J.; Frederick, J. E. Factors affecting the detection of trends: Statistical considerations and applications to environmental data. *J. Geophys. Res.* **1998**, *103*, 17149−17161.
(31) Chandler, R.; Scott, M. *Statistical Methods for Trend Detection and Analysis in the Environmental Sciences*; John Wiley & Sons, 2011.
(32) Kendall, M. G. *Rank Correlation Methods*; Charles Griffin: London, 1955.
(33) Theil, H. A rank-invariant method of linear and polynomial regression analysis, I. *Proc. Kon Ned Akad v. Wetensch A* **1950**, *53*, 386−392.
(34) Sen, P. K. Estimates of the regression coefficient based on Kendall's tau. *J. Am. Stat. Assoc.* **1968**, *63*, 1379−1389.
(35) GBD 2017 Risk Factor Collaborators. Global Burden of Diseases, Global, regional, and national comparative risk assessment of 84 behavioural, environmental and occupational, and metabolic risks or clusters of risks for 195 countries and territories, 1990−2017: a systematic analysis for the Global Burden of Disease Study 2017. *Lancet* **2018**, *392*, 1923−1994.
(36) Seltzer, K. M.; Shindell, D. T.; Malley, C. S. Measurement-based assessment of health burdens from long-term ozone exposure in the United States, Europe, and China. *Environ. Res. Lett.* **2018**, *13*, 104018.
(37) Gao, M.; Beig, G.; Song, S.; Zhang, H.; Hu, J.; Ying, Q.; Liang, F.; Liu, Y.; Wang, H.; Lu, X.; Zhu, T.; Carmichael, G. R.; Nielsen, C. P.; McElroy, M. B. The impact of power generation emissions on ambient PM2.5 pollution and human health in China and India. *Environ. Int.* **2018**, *121*, 250−259.
(38) Xu, J.; Tie, X.; Gao, W.; Lin, Y.; Fu, Q. Measurement and model analyses of the ozone variation during 2006 to 2015 and its response to emission change in megacity Shanghai, China. *Atmos. Chem. Phys.* **2019**, *19*, 9017−9035.
(39) Strode, S. A.; Ziemke, J. R.; Oman, L. D.; Lamsal, L. N.; Olsen, M. A.; Liu, J. Global changes in the diurnal cycle of surface ozone. *Atmos. Environ.* **2019**, *199*, 323−333.
(40) Yan, Y.; Lin, J.; Pozzer, A.; Kong, S.; Lelieveld, J. Trend reversal from high-to-low and from rural-to-urban ozone concentrations over Europe. *Atmos. Environ.* **2019**, *213*, 25−36.
(41) Huang, J.; Pan, X.; Guo, X.; Li, G. Health impact of China's Air Pollution Prevention and Control Action Plan: an analysis of national air quality monitoring and mortality data. *Lancet Planetary Health* **2018**, *2*, e313−e323.
(42) Silva, R. A.; West, J. J.; Zhang, Y.; Anenberg, S. C.; Lamarque, J.-F.; Shindell, D. T.; Collins, W. J.; Dalsoren, S.; Faluvegi, G.; Folberth, G.; Horowitz, L. W.; Nagashima, T.; Naik, V.; Rumbold, S.; Skeie, R.; Sudo, K.; Takemura, T.; Bergmann, D.; Cameron-Smith, P.; Cionni, I.; Doherty, R. M.; Eyring, V.; Josse, B.; MacKenzie, I. A.; Plummer, D.; Righi, M.; Stevenson, D. S.; Strode, S.; Szopa, S.; Zeng, G. Global premature mortality due to anthropogenic outdoor air pollution and the contribution of past climate change. *Environ. Res. Lett.* **2013**, *8*, 034005.
(43) Liu, H.; Liu, S.; Xue, B.; Lv, Z.; Meng, Z.; Yang, X.; Xue, T.; Yu, Q.; He, K. Ground-level ozone pollution and its health impacts in China. *Atmos. Environ.* **2018**, *173*, 223−230.
(44) Feng, Z.; Hu, E.; Wang, X.; Jiang, L.; Liu, X. Ground-level O3 pollution and its impacts on food crops in China: a review. *Environ. Pollut.* **2015**, *199*, 42−8.
(45) Yue, X.; Unger, N.; Harper, K.; Xia, X.; Liao, H.; Zhu, T.; Xiao, J.; Feng, Z.; Li, J. Ozone and haze pollution weakens net primary productivity in China. *Atmos. Chem. Phys.* **2017**, *17*, 6073−6089.
(46) Feng, Z.; De Marco, A.; Anav, A.; Gualtieri, M.; Sicard, P.; Tian, H.; Fornasier, F.; Tao, F.; Guo, A.; Paoletti, E. Economic losses due to ozone impacts on human health, forest productivity and crop yield across China. *Environ. Int.* **2019**, *131*, 104966.
(47) Feng, Z.; Kobayashi, K.; Li, P.; Xu, Y.; Tang, H.; Guo, A.; Paoletti, E.; Calatayud, V. Impacts of current ozone pollution on wheat yield in China as estimated with observed ozone, meteorology and day of flowering. *Atmos. Environ.* **2019**, *217*, 116945.
(48) Zheng, B.; Tong, D.; Li, M.; Liu, F.; Hong, C.; Geng, G.; Li, H.; Li, X.; Peng, L.; Qi, J.; Yan, L.; Zhang, Y.; Zhao, H.; Zheng, Y.; He, K.; Zhang, Q. Trends in China's anthropogenic emissions since 2010 as the consequence of clean air actions. *Atmos. Chem. Phys.* **2018**, *18*, 14095−14111.
(49) Jin, X.; Holloway, T. Spatial and temporal variability of ozone sensitivity over China observed from the Ozone Monitoring Instrument. *J. Geophys. Res.* **2015**, *120*, 7229−7246.

https://dx.doi.org/10.1021/acs.estlett.0c00171
Environ. Sci. Technol. Lett. 2020, 7, 240−247

(50) Ou, J.; Yuan, Z.; Zheng, J.; Huang, Z.; Shao, M.; Li, Z.; Huang, X.; Guo, H.; Louie, P. K. Ambient Ozone Control in a Photochemically Active Region: Short-Term Despiking or Long-Term Attainment? *Environ. Sci. Technol.* **2016**, *50*, 5720−8.
(51) Li, Q.; Zhang, L.; Wang, T.; Wang, Z.; Fu, X.; Zhang, Q. New" Reactive Nitrogen Chemistry Reshapes the Relationship of Ozone to Its Precursors. *Environ. Sci. Technol.* **2018**, *52*, 2810−2818.
(52) Zhai, S.; Jacob, D. J.; Wang, X.; Shen, L.; Li, K.; Zhang, Y.; Gui, K.; Zhao, T.; Liao, H. Fine particulate matter (PM2.5) trends in China, 2013−2018: separating contributions from anthropogenic emissions and meteorology. *Atmos. Chem. Phys.* **2019**, *19*, 11031−11041.
(53) Zhang, Q.; Zheng, Y.; Tong, D.; Shao, M.; Wang, S.; Zhang, Y.; Xu, X.; Wang, J.; He, H.; Liu, W.; Ding, Y.; Lei, Y.; Li, J.; Wang, Z.; Zhang, X.; Wang, Y.; Cheng, J.; Liu, Y.; Shi, Q.; Yan, L.; Geng, G.; Hong, C.; Li, M.; Liu, F.; Zheng, B.; Cao, J.; Ding, A.; Gao, J.; Fu, Q.; Huo, J.; Liu, B.; Liu, Z.; Yang, F.; He, K.; Hao, J. Drivers of improved PM2.5 air quality in China from 2013 to 2017. *Proc. Natl. Acad. Sci. U. S. A.* **2019**, *116*, 24463.
(54) Lou, S.; Liao, H.; Zhu, B. Impacts of aerosols on surface-layer ozone concentrations in China through heterogeneous reactions and changes in photolysis rates. *Atmos. Environ.* **2014**, *85*, 123−138.
(55) Zhao, Z.; Wang, Y. Influence of the West Pacific subtropical high on surface ozone daily variability in summertime over eastern China. *Atmos. Environ.* **2017**, *170*, 197−204.
(56) Ma, M.; Gao, Y.; Wang, Y.; Zhang, S.; Leung, L. R.; Liu, C.; Wang, S.; Zhao, B.; Chang, X.; Su, H.; Zhang, T.; Sheng, L.; Yao, X.; Gao, H. Substantial ozone enhancement over the North China Plain from increased biogenic emissions due to heat waves and land cover in summer 2017. *Atmos. Chem. Phys.* **2019**, *19*, 12195−12207.
(57) Gong, C.; Liao, H. A typical weather pattern for ozone pollution events in North China. *Atmos. Chem. Phys.* **2019**, *19*, 13725−13740.
(58) Yang, L.; Luo, H.; Yuan, Z.; Zheng, J.; Huang, Z.; Li, C.; Lin, X.; Louie, P. K. K.; Chen, D.; Bian, Y. Quantitative impacts of meteorology and precursor emission changes on the long-term trend of ambient ozone over the Pearl River Delta, China, and implications for ozone control strategy. *Atmos. Chem. Phys.* **2019**, *19*, 12901−12916.
(59) Yin, Z.; Cao, B.; Wang, H. Dominant patterns of summer ozone pollution in eastern China and associated atmospheric circulations. *Atmos. Chem. Phys.* **2019**, *19*, 13933−13943.
(60) Han, H.; Liu, J.; Shu, L.; Wang, T.; Yuan, H. Local and synoptic meteorological influences on daily variability in summertime surface ozone in eastern China. *Atmos. Chem. Phys.* **2020**, *20*, 203−222.
(61) Gaudel, A.; Cooper, O. R.; Ancellet, G.; Barret, B.; Boynard, A.; Burrows, J. P.; Clerbaux, C.; Coheur, P. F.; Cuesta, J.; Cuevas, E.; Doniki, S.; Dufour, G.; Ebojie, F.; Foret, G.; Garcia, O.; Granados Muños, M. J.; Hannigan, J. W.; Hase, F.; Huang, G.; Hassler, B.; Hurtmans, D.; Jaffe, D.; Jones, N.; Kalabokas, P.; Kerridge, B.; Kulawik, S. S.; Latter, B.; Leblanc, T.; Le Flochmoën, E.; Lin, W.; Liu, J.; Liu, X.; Mahieu, E.; McClure-Begley, A.; Neu, J. L.; Osman, M.; Palm, M.; Petetin, H.; Petropavlovskikh, I.; Querel, R.; Rahpoe, N.; Rozanov, A.; Schultz, M. G.; Schwab, J.; Siddans, R.; Smale, D.; Steinbacher, M.; Tanimoto, H.; Tarasick, D. W.; Thouret, V.; Thompson, A. M.; Trickl, T.; Weatherhead, E.; Wespes, C.; Worden, H. M.; Vigouroux, C.; Xu, X.; Zeng, G.; Ziemke, J. Tropospheric Ozone Assessment Report: Present-day distribution and trends of tropospheric ozone relevant to climate and global atmospheric chemistry model evaluation. *Elem Sci. Anth* **2018**, *6*, 39.

https://dx.doi.org/10.1021/acs.estlett.0c00171
Environ. Sci. Technol. Lett. 2020, 7, 240−247